

MIRART, a line-by-line code for infrared atmospheric radiation computations including derivatives

F. Schreier and U. Böttger

*DLR - Remote Sensing Technology Institute
Oberpfaffenhofen, 82234 Wessling, Germany*

Received December 16, 2002

A suite of programs MIRART (Modular Infrared Atmospheric Radiance and Transmission) for high resolution infrared atmospheric radiative transfer calculations has been developed with emphasis on efficient and reliable numerical algorithms and a modular approach appropriate for simulation and/or retrieval in a variety of applications. The code has been carefully tested in the framework of two extensive inter-comparisons. Molecular weighting functions are implemented by means of automatic differentiation.

Introduction

In recent years the widespread use of high resolution spectrometers for groundbased, airborne, or spaceborne atmospheric remote sensing has resulted in an increased interest in Line-by-Line (LbL) radiative transfer modeling. For example, our institute operates an airborne far infrared heterodyne spectrometer,¹ and Fourier Transform Spectrometer (FTS) for infrared laboratory spectroscopy of molecules,² groundbased measurements of atmospheric trace gases, and (airborne and laboratory) spectroscopy of jet engine exhausts.³ A combination of FTS and imaging spectrometer is currently in preparation for airborne observations of high temperature events (wild fires, volcanoes, etc.⁴).

An essential prerequisite for the analysis of high resolution spectra as well as for theoretical studies such as retrieval assessments is a flexible, yet efficient radiative transfer code. Furthermore, as the retrieval of atmospheric parameters is in general a nonlinear optimization problem (inverse problem), the retrieval code has to be closely connected to the radiative transfer code (forward model).

The recent increase in computational power has greatly helped to develop LbL radiative transfer codes. Although a variety of general purpose LbL codes has been developed in the past decades, i.e., FASCOD⁵ and GENLN2,⁶ a new code has been found to be desirable because implementation of these sophisticated LbL programs in retrieval algorithms is generally a non-trivial task. Furthermore derivatives with respect to the unknown profiles are often not available or at least difficult to access.

1. Basics of Infrared Atmospheric Radiative Transfer

The intensity (radiance) I at wavenumber ν received by an instrument at position $s = 0$ can be

described by the integral form of the equation of radiative transfer (neglecting scattering and assuming local thermodynamic equilibrium)⁷

$$I(\nu) = I_{\infty}(\nu) \tau(\nu; \infty) - \int_0^{\infty} ds' B[\nu, T(s')] \frac{\partial \tau(\nu; s')}{\partial s'}, \quad (1)$$

where I_{∞} is a background contribution, (e.g., the radiation emitted by the Earth's surface in case of downlooking instruments) and B is the Planck function at temperature T ,

$$B(\nu, T) = 2hc^2\nu^3 / [\exp(hc\nu/k_B T) - 1], \quad (2)$$

with c , h , k_B denoting speed of light, Planck and Boltzmann constant, respectively. The monochromatic transmission τ is given according to Beer's law by

$$\tau(\nu; s) = \exp \left[- \int_0^s \alpha(\nu, s') ds' \right], \quad (3)$$

$$\alpha(\nu; s) = \sum_m k_m[\nu, \rho(s), T(s)] n_m(s) + \alpha^{(c)}(\nu, s), \quad (4)$$

where α is the volume absorption coefficient, k_m and n_m are the absorption cross section and density of molecule m , and $\alpha^{(c)}$ is the continuum absorption coefficient. Instrumental effects are taken into account by convolution with appropriate Instrumental Line Shape (ILS) and Field of View (FoV) functions.

In general, the molecular cross section is obtained by summing over the contributions from many lines, $k_m = \sum_l k_m^{(l)}$. For an individual line the cross section is the product of the temperature dependent line strength $S(T)$ and a normalized line shape function $g(\nu)$ describing the broadening mechanism(s),

$$k(\nu, s) = S[T(s)] g[\nu, \rho(s), T(s)]. \quad (5)$$

In the atmosphere the combined effect of pressure broadening (half width proportional to pressure, $\gamma_L \sim p$), corresponding to a Lorentzian line shape

$$g_L(\nu) = \frac{\gamma_L/\pi}{(\nu - \nu_0)^2 + \gamma_L^2}, \quad (6)$$

and Doppler broadening, corresponding to a Gaussian line shape

$$g_D(\nu) = \frac{1}{\gamma_D} \left(\frac{\ln 2}{\pi} \right)^{1/2} \exp \left[-\ln 2 \left(\frac{\nu - \nu_0}{\gamma_D} \right)^2 \right], \quad (7)$$

with $\gamma_D \sim \nu_0 \sqrt{T}$ that can be represented by a Voigt line profile $g_V(\nu) = g_L \otimes g_D$.

2. Numerical aspects

Given the variety of applications MIRART has been designed for arbitrary observation geometry, FoV, and ILS. The following subsections discuss some distinct features.

2.1. Voigt function

The convolution integral defining the Voigt profile

$$g_V(\nu) = \frac{\sqrt{\ln 2/\pi}}{\gamma_D} K(x, y), \quad (8)$$

$$K(x, y) = \frac{y}{\pi} \int_{-\infty}^{\infty} \frac{e^{-t^2}}{(x-t)^2 + y^2} dt, \quad (9)$$

cannot be evaluated in closed form and therefore has to be computed numerically. Most modern algorithms rely on approximations for the complex error function $w(z)$ whose real part represents the Voigt function $K(x, y) = \Re[w(x + iy)]$. Here the dimensionless variables x, y are defined in terms of the distance from the line center ν_0 and the Lorentzian and Doppler half widths, $x = \sqrt{\ln 2} (\nu - \nu_0) / \gamma_D$ and $y = \sqrt{\ln 2} \gamma_L / \gamma_D$. Rational approximations are known to give accurate and efficient algorithms for a large class of functions. For the calculation of the complex error function MIRART uses an optimized combination⁸ of algorithms developed by Humlicek⁹ and Hui et al.¹⁰

2.2. Molecular absorption cross sections

The line-by-line calculation of the cross sections is generally the most time consuming part of high resolution radiative transfer codes, and a large variety of optimization schemes has been developed.^{5,6,11,12} In MIRART the wavenumber grid is chosen individually for each altitude level and molecule. Furthermore, a coarse grid is used for contributions of lines outside the spectral region of interest, and line center contributions are calculated on a fine spectral grid.

Molecular cross sections are calculated with spectroscopic data from HITRAN,¹³ HITEMP,¹⁴ GEISA,¹⁵ or JPL¹⁶ dataset(s). In addition to the line

contributions continua are implemented for water, carbon dioxide, oxygen, and nitrogen.^{17,18}

2.3. Line strengths temperature dependence

The conversion of line strengths from temperature T_0 , i.e., the reference temperature of the spectroscopic line parameter data base, to the actual temperature \hat{O} is calculated according to the scheme used in the ATMOS software¹⁹

$$S(T) = S(T_0) \frac{Q(T_0) \exp(-E_l/kT) (1 - \exp(-hc\nu_0/kT))}{Q(T) \exp(-E_l/kT_0) (1 - \exp(-hc\nu_0/kT_0))}. \quad (10)$$

$Q(T)$ is the product of rotational and vibrational partition functions, $Q = Q_{\text{rot}} Q_{\text{vib}}$ with

$$Q_{\text{rot}}(T) = Q_{\text{rot}}(T_0) (T/T_0)^\beta, \quad (11)$$

$$Q_{\text{vib}}(T) = \prod_{i=1}^N [1 - \exp(-hc\nu_i/kT)]^{-d_i}, \quad (12)$$

where β is the temperature coefficient of the rotational partition function and N is the number of vibrational modes with wavenumbers ν_i and degeneracies d_i .

2.4. Path integration

The solution of Schwarzschild's equation (1) and Beer's law (3) requires the integration of spatially varying quantities (given only for a set of discrete altitude points) along the line of sight. The standard approach is to divide the atmosphere in a series of homogeneous layers described by "mean" temperature, pressure, and concentrations. Using this Curtis–Godson approximation, the total transmission is the product of all layer transmissions and the radiance is calculated recursively.

Alternatively, the integrals in Eqs. (1) and (3) can be calculated using standard numerical quadrature schemes; for example, using an n -point quadrature rule, the optical depth in Eqs. (3) is given generally by

$$\tau = \int_{s_b}^{s_e} \alpha(s) ds = \sum_j w_j \alpha(s_j), \quad (13)$$

where the weights w_j and nodes s_j are defined by the chosen quadrature rule. MIRART has implemented a trapezoid quadrature scheme, the method of overlapping parabolas,²⁰ or a quadrature using the piecewise cubic Hermite interpolant (PCHIP) of the integrand²¹ (see Fig. 1). Note that these quadrature rules work for arbitrarily spaced abscissas s . For a slant path geometry with zenith angle θ in a flat atmosphere the altitude grid points z_i and the path grid points s_j are essentially equivalent except for a $\cos(\theta)$ factor. For limb path geometries a mapping of the altitude dependent atmospheric profiles to the distance s along the line of sight is performed, e.g., $T(s) = T(z(s))$, etc.

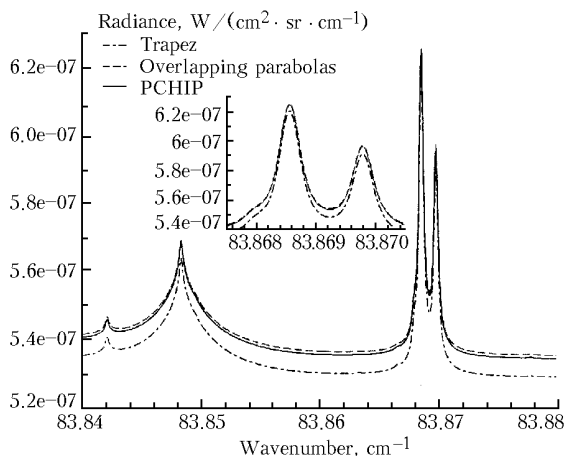


Fig. 1. Comparison of far infrared spectrum in the vicinity of the OH triplet at 83.869 cm^{-1} for different quadrature rules: Limb path with observer at 50 km, tangent at 20 km. H_2I , I_3 , I_1 , I_2 , and empirical FIRS continuum. Voigt line shape with cutoff at 2 cm^{-1} from line center. The large feature at 83.848 cm^{-1} is due to ozone. (The insert shows a zoom of the OH triplet, however, the rather weak third line of the triplet is not visible.) Execution time for piecewise cubic Hermite quadrature is significantly longer than for trapezoid or overlapping parabola.

2.5. Optimization of the overlapping parabola quadrature

For overlapping parabola quadrature MIRART utilizes the Fortran 77 subroutine AVINT of the SLATEC²² library. In general (cf. Fig. 1) there is a good agreement of spectra obtained with AVINT and PCHIP quadrature, whereas spectra calculated with trapezoid quadrature show slight deviations. On the other hand, although AVINT is faster than PCHIP, it is still considerably slower than trapezoid quadrature.

However, the relative simplicity of the overlapping parabola quadrature made an optimization straightforward, resulting in an accelerated algorithm only slightly slower than trapezoid quadrature. Some reorganization of the code already resulted in considerable speed up: moving IF statements outside a DO loop, avoiding unnecessary divisions, and skipping repeated checks of input parameters. Furthermore, calculation of the radiance (1) also requires knowledge of the transmission $\tau(v, s')$ as a function of distance to the observer s' , i.e., for all path grid points s_j between observer and end-of-path. In this case the weights w_j can be calculated once and the stepwise quadrature from a fixed starting point to a sequence of end points s_j can be formulated as a matrix-vector product.

2.6. Implementation

The current version of MIRART is written in Fortran 77 using some Fortran 90 extensions, utilizing

open source libraries (SLATEC²² and BLAS²³) as far as possible.

Program execution is controlled by a file formatted using Fortran Namelist allowing format-free input. All data except for a few fundamental constants such as π are read from external files; in particular, molecular parameters such as mass, vibrational frequencies, etc. are read from file, hence "new" molecules can be added without recompilation.

3. Verification

Among the most important, yet difficult steps in program development are validation and verification. Unfortunately, a closed analytic solution of the radiative transfer equations is not available for realistic conditions, and hence a comparison of numerical results with reference values is not feasible. Clearly testing code against analytical results is mandatory for intermediate quantities, e.g., cross sections, but this obviously does not prove the correctness and consistency of the whole code. Comparing computed spectra with experimental measurements is difficult due to the incomplete knowledge of the atmosphere and inaccuracy of spectroscopic data. Thus, this approach is essentially limited to laboratory measurements for a homogeneous gas cell, i.e., it does not test the correctness of the numerical solution of the path integrals in Eqs. (1) and (3).

Hence, the standard approach to verification of LbL codes relies on cross checks against similar codes. Recently MIRART participated in two extensive intercomparisons.

3.1. Advanced MIPAS Level 2 Data Analysis (AMIL2DA)

In order to assess the consistency of level 2 data generated from measurements by the MIPAS Fourier transform limb emission spectrometer onboard the ENVISAT satellite, the AMIL2DA project aims at careful comparison and characterization of algorithms and data analysis strategies used by different European groups. An essential step of this project is a cross comparison of the radiative transfer forward models to be used as a part of the group's MIPAS data processing.²⁴ The intercomparison was organized as a series of exercises, starting from simple settings proving basic functionalities and proceeding to more complex and realistic scenarios. Accordingly, the first exercises considered the transmission of a single N_2O line for different pressures and temperatures, hence, testing line shape computation and line strength conversion. In a second set of exercises radiance spectra for a limb viewing geometry with instrumental effects have been intercompared. Figure 2 shows a comparison of a limb emission spectrum, revealing deviations well below one percent.

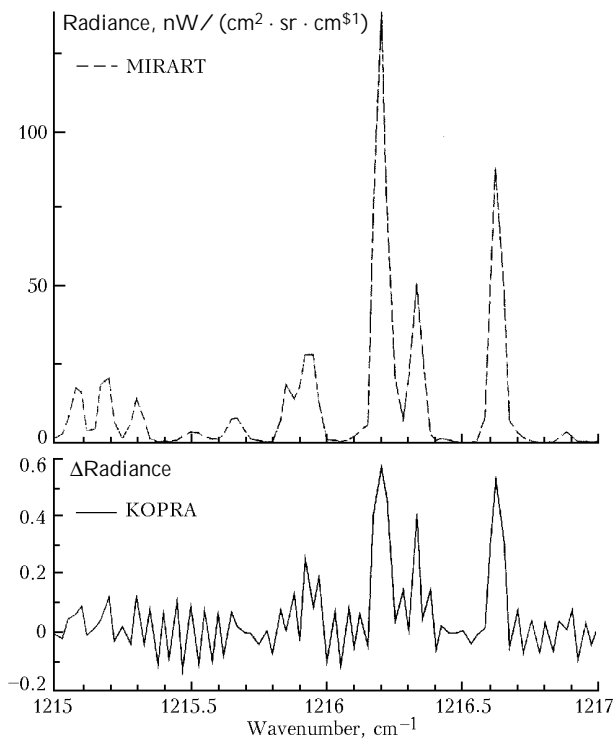


Fig. 2. AMIL2DA Forward model intercomparison (Exercise 20): KOPRA line-by-line code³¹ and MIRART. Limb view with tangent altitude 40 km, apodized FTS instrument line shape, finite field-of-view. H₂O, CO₂, O₃, N₂O, and CH₄; CKD-continuum.⁵

3.2. International radiative transfer modeling workshop 2001 (IRTMW01)

A major objective of IRTMW01 was the intercomparison of radiative transfer codes in the microwave spectral domain.²⁵ Similar to the AMIL2DA intercomparison, it was organized in a series of progressively more sophisticated "cases", starting with an assessment of Voigt line shape and molecular absorption coefficient calculations. As for the corresponding AMIL2DA exercises, MIRART exhibited slight deviations for spectra at temperatures different from the database reference temperature that have been attributed to the use of different line strengths conversion approaches.

The purpose of case 3 was to check the correct implementation of the radiative transfer algorithm, i.e., the solution of the integrals in Eqs. (1) and (3). In order to allow discrimination of different sources of possible deviations between the models, absorption coefficients $\alpha(\nu, z)$ have been pre-calculated by the University of Bremen group and used as common input. Case 4 was aiming to test the entire computational chain of the codes including LbL calculation, continuum corrections, and path quadrature. Geometries and instrument settings were identical to case 3, thus, changes from case 3 spectra to case 4 spectra have to come from differences in the input data or from differences in the cross section and absorption coefficient calculations.

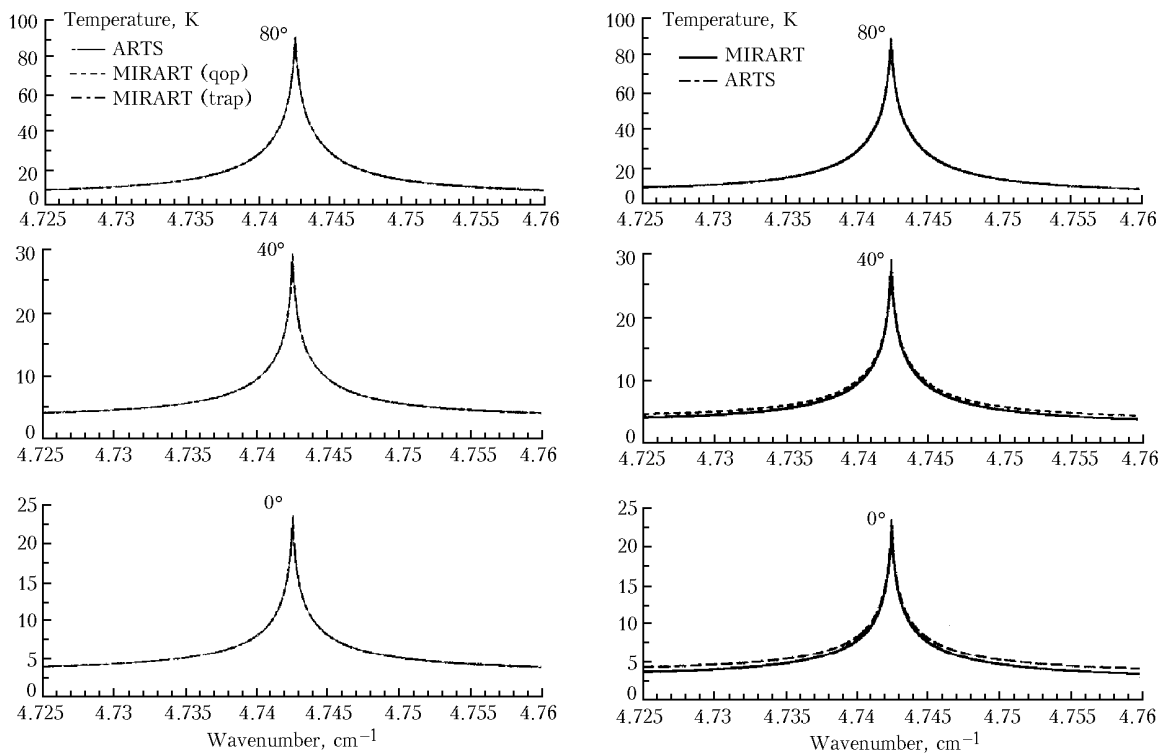


Fig. 3. IRTMW01 intercomparison: case 3 (left) and 4 (right) up-looking: ARTS line-by-line code (University of Bremen) vs. MIRART. (On the left "qop" and "trap" refers to "quadrature with overlapping parabolas" and "trapezoid quadrature", respectively, cf. subsection 3.4). \bar{T}_3 and O₂, perfect antenna (i.e., infinitesimal FoV), single side band receiver with Gaussian ILS function with half width 0.25 MHz.

The intercomparison was performed for different geometries, and for ideal monochromatic spectra as well as ILS and FoV convolved spectra. Figure 3 shows the results for the uplooking geometry: Whereas case 3 spectra do not yield visible differences, slight deviations show up in case 4 for small zenith angles. Similar results were also found for the case 3 and case 4 down looking and limb viewing exercises.

4. Weighting functions

Remote sensing of the atmosphere by high-resolution spectroscopy is a well established technique allowing determination of temperature, pressure, and constituent profiles by inversion of the integral equation of radiative transfer. Because, in general, the relation between the unknown profile and the spectrum (Eqs. (1), (3)) is nonlinear, the inversion has to be accomplished by Newtonian iteration based on linearization. In many cases the differentiation to compute the Jacobian or "weighting functions" is performed by finite difference numerical derivatives, and thus frequently constitutes the most time consuming part of the retrieval. And, even more serious, the appropriate amount of perturbation is difficult to predict (truncation and/or cancellation errors, see Ref. 26).

Analytical means of weighting function calculations are therefore advantageous both for computational efficiency and accuracy. However, calculating derivatives manually and implementing these in a moderately large codes is tedious and error prone.

Automatic differentiation provides a pleasant alternative to quickly generate derivative-enhanced versions of computer codes. Automatic differentiation techniques^{27,28} are based on the fact that every model implemented as a computer program is essentially formulated in terms of elementary operations (sums, products, powers) and elementary functions. In contrast to integration, differentiation is based on a few simple recipes such as the chain rule, and these can be performed automatically by some kind of precompiler, taking a computer code as input and delivering a code that additionally produces derivatives with respect to some chosen variables. A number of automatic differentiation tools are available for Fortran, C, etc.; here we used the ADIFOR system²⁹ for automatic differentiation of Fortran 77 code.

The first step is to identify the function to be differentiated, usually corresponding to a subroutine in case of Fortran. The Jacobians required for the nonlinear least squares solver in atmospheric retrievals are the derivatives of the radiance vector with respect to the discretized representation (vector) of the atmospheric profile. Because least squares aims to minimize the residual between observed and modeled spectra, instrumental effects have to be included in the model. Hence the "top-level subroutine" to be differentiated includes path quadrature as well as convolution of the monochromatic spectrum with ILS and FoV. Furthermore, the independent (here molecular

concentration) and dependent (instrumentally modified radiance) variables of the function with respect to differentiation have to be identified. Because Fortran 77 does not allow dynamic memory allocation, ADIFOR also requires to specify an upper bound on the size of the gradient object, which can be set to the maximum number of altitude levels used for the atmospheric profiles. This information is collected in an ADIFOR "script file" as shown in Fig. 4.

```
AD_TOP      = schwarzschild_ils_fov
AD_IVARS    = Density
AD_DVARS    = Radiance
AD_PMAX     = 50
```

Fig. 4. ADIFOR script file used for MIRART molecular concentration weighting functions.

The next step is to generate a "composition file", i.e., a listing of all source files making up the program, cf. Fig. 5. This listing essentially contains a main program and all subprograms called by the top-level subroutine thus comprising the entire code necessary to evaluate the dependent variable(s) as a function of the independent variable(s). It is not required to submit the entire code to ADIFOR. In the case of molecular weighting functions the LbL section is irrelevant and can be omitted. Likewise, it is not necessary to include the actual main program, a dummy main program that only contains a call to the top-level subroutine and appropriate declarations is hence sufficient.

```
dummy_main.f
schwarzschild_ils_fov.f
schwarzschild.f
convolve_ils.f
convolve_fov.f
.....
```

Fig. 5. Excerpt of the ADIFOR composition file used for MIRART weighting functions (note that this excerpt is for illustrative purposes only and the names do not correspond to the actual source files; actually our composition file contains more than 100 routines).

Invoking ADIFOR now generates the derivative code for the top-level subroutine and for all relevant subroutines called by it (directly or indirectly). Note that in the new code statements, involving the independent, dependent, or intermediate variables, are augmented by corresponding statements to compute the derivative. Thus, the argument list of all augmented subroutines will be extended by derivative variables, and the routine or main program calling the top-level subroutine has to be adjusted appropriately. Furthermore, a so-called seed matrix has to be introduced indicating with respect to which elements of the vector (or matrix) derivatives are to be calculated. Finally these new routines along with any other modules necessary to form a complete program are compiled and linked.

In Fig. 6 limb view $H_2\hat{I}$ weighting functions computed with the automatic derivatives enhanced

forward model and by two point finite differences are compared, clearly indicating the problem of choosing the right perturbation for finite difference approximations. Computing time for a limb sequence of radiance and Jacobians has increased by about a factor three comparative to the pure radiance calculation, i.e., there is a significant computational gain as compared to the finite difference approach for a Jacobian with 20 columns.

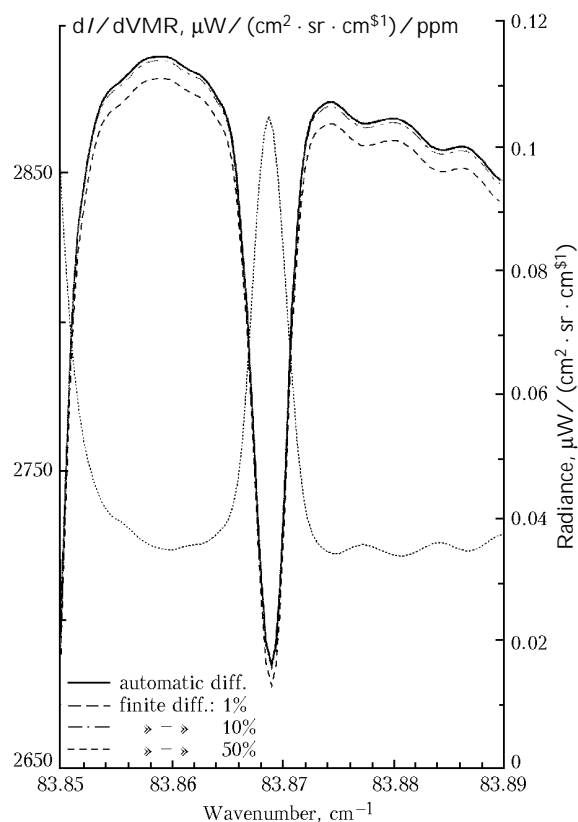


Fig. 6. Comparison of Jacobian for H_2O at 25 km computed by automatic differentiation and by finite differences. Limb view to 25 km tangent height; H_2O , O_3 , HO_2 , and OH, and CKD continuum; line parameters from SAO database. Gaussian FoV with 1 km half width. FTS with MOPD = 300 cm, Norton–Beer medium apodization. The dot-dashed curve with the axis on the right shows the radiance $I(\nu)$; the strong signature at 83.87 cm^{-1} is due to the OH line triplet, cf. Fig. 1.

5. Future developments

The Modular InfraRed Atmospheric Radiance and Transmission (MIRART) LbL code for high resolution radiative transfer computations has been presented with an emphasis on its numerical implementation. In particular, automatic differentiation has been used to generate code for exact molecular weighting functions. Current work focuses on implementation of derivatives with respect to further variables (temperature) and integration in the "Virtual lab".³⁰

Acknowledgment

The authors would like to thank A. Doicu, M. Hess, and J. Mendrok for many helpful discussions. AMIL2DA is a Shared Cost Action within the RTD generic activities of the 5th FP EESD Programme of the European Commission, project EVG1–CT–1999–00015.

References

1. N. Englert, A. Schimpf, M. Birk, F. Schreier, M. Krocka, R.G. Nitsche, R.U. Titz, and M.E. Summers, *The 2.5 THz heterodyne spectrometer THOMAS: Measurement of OH in the middle atmosphere and comparison with photochemical model results*, *J. Geophys. Res.* **105**, 22211–22223 (2000).
2. M. Birk, D. Hausamann, F. Schreier, and G. Wagner, *High resolution infrared laboratory spectroscopy of atmospheric constituents at DLR*, in: J. Demaison, K. Sarka, and E.A. Cohen, eds., *Spectroscopy from Space*, Vol. 20 of *NATO Science Series II* (Kluwer Academic Publishers, 2001), pp. 219–233.
3. P. Haschberger and E. Lindermeir, *Spectrometric inflight measurement of aircraft exhaust emissions*, *J. Geophys. Res.* **101**, 25995–26006 (1996).
4. V. Tank, P. Haschberger, K. Bochtcr, D. Oertel, K. Beier, F. Schreier, M. Birk, E. Lindermeir, and G. Wagner, *Spectroscopic measurements from space with the FOCUS sensor system to analyse gas and smoke properties of high temperature events*, in: J. Demaison, K. Sarka, and E.A. Cohen, eds., *Spectroscopy from Space*, Vol. 20 of *NATO Science Series II* (Kluwer Academic Publishers, 2001), pp. 259–273.
5. S.A. Clough, F.X. Kneizys, G.P. Anderson, E.P. Shettle, J.H. Chetwynd, L.W. Abreu, L.A. Hall, and R.D. Worsham, *FASCOD3: spectral simulation*, in: J. Lenoble and J.F. Geleyn, eds., *IRS'88: Current Problems in Atmospheric Radiation* (A. Deepak Publishing, 1988), pp. 372–375.
6. D.P. Edwards, *Atmospheric transmittance and radiance calculations using line-by-line computer models*, *Proc. SPIE* **928**, *Modelling of the Atmosphere*, 94–116 (1988).
7. Kuo-Nan Liou, *An Introduction to Atmospheric Radiation* (Academic Press, Orlando, 1980).
8. F. Schreier, *The Voigt and complex error function: A comparison of computational methods*, *J. Quant. Spectrosc. Radiat. Transfer* **48**, 743–762 (1992).
9. J. Humlicek, *Optimized computation of the Voigt and complex probability function*, *J. Quant. Spectrosc. Radiat. Transfer* **27**, 437–444 (1982).
10. A.K. Hui, B.H. Armstrong, and A.A. Wray, *Rapid computation of the Voigt and complex error functions*, *J. Quant. Spectrosc. Radiat. Transfer* **19**, 509–516 (1978).
11. B.A. Fomin, *Effective interpolation technique for line-by-line calculation of radiation absorption in gases*, *J. Quant. Spectrosc. Radiat. Transfer* **53**, 663–669 (1995).
12. M. Kuntz and M. Hopfner, *Efficient line-by-line calculation of absorption coefficients*, *J. Quant. Spectrosc. Radiat. Transfer* **63**, 97–114 (1999).
13. L.S. Rothman, C.P. Rinsland, A. Goldman, S.T. Massie, D.P. Edwards, J.-M. Flaud, A. Perrin, C. Camy-Peyret, V. Dana, J.-Y. Mandin, J. Schroeder, A. McCann, R.R. Gamache, R.B. Wattson, K. Yoshino, K.V. Chance, K.W. Jucks, L.R. Brown, V. Ncmitchinov, and P. Varanasi, *The HITRAN molecular spectroscopic database and HAWKS (Hitran Atmospheric Workstation): 1996 edition*, *J. Quant. Spectrosc. Radiat. Transfer* **60**, 665–710 (1998).

14. L.S. Rothman, R.B. Wattson, R.R. Gamache, J. Schroeder, and A. McCann, *HITRAN HAWKS and HITEMP high temperature molecular database*, Proc. SPIE **2471**, 105–111 (1995).
15. N. Jacquinet-Husson, E. Arie, J. Ballard, A. Barbe, G. Bjoeraker, B. Bonnet, L.R. Brown, C. Camy-Peyret, J.P. Champion, A. Chedin, A. Chursin, C. Clerbaux, G. Duxbury, J.-M. Flaud, N. Fourrie, A. Fayt, G. Graner, R. Gamache, A. Goldman, VI. Golovko, G. Guelachvili, J.M. Hartmann, J.C. Hilico, J. Hillman, G. Lefevre, E. Lcllouch, S.N. Mikhailenko, O.V. Naumenko, V. Ncmitchinov, D.A. Newnham, A. Nikitin, J. Orphal, A. Perrin, D.C. Reuter, C.P. Rinsland, L. Rosenmann, L.S. Rothman, N.A. Scott, J. Selby, L.N. Siniitsa, J.M. Sirota, A.M. Smith, K.M. Smith, VI.G. Tyuterev, R.H. Tipping, S. Urban, P. Varanasi, and M. Weber, *The 1997 spectroscopic GEISA databank*, J. Quant. Spectrosc. Radiat. Transfer **62**, 205–254 (1999).
16. H.M. Pickett, R.L. Poynter, E.A. Cohen, M.L. Delitsky, J.C. Pearson, and H.S.P. Muller, *Submillimeter, millimeter, and microwave spectral line catalog*, J. Quant. Spectrosc. Radiat. Transfer **60**, 883–890 (1998).
17. S.A. Clough, F.X. Kneizys, and R. Davies, *Line shape and the water vapor continuum*, Atmos. Res. **23**, 229–241 (1989).
18. G. Echle, *Study of the retrieval of atmospheric trace gas profiles from infrared spectra*, Draft report on task 1: Continuum, ESA Contract 12055/96/NL/CN, 1997.
19. R.H. Norton and C.P. Rinsland, *ATMOS data processing and science analysis methods*, Appl. Opt. **30**, 389–400 (1991).
20. Ph.J. Davis and Ph. Rabinowitz, *Numerical Integration* (Blaisdell Publishing Company, 1967).
21. D. Kahaner, C. Moler, and S. Nash, *Numerical Methods and Software* (Prentice-Hall, Englewood Cliffs, NJ, 1989).
22. SLATEC. Common Mathematical Library (Version 4.1). Available from NetLib, <http://www.netlib.org/>, July 1993.
23. C.L. Lawson, R.J. Hanson, D.R. Kincaid, and F.T. Krogh, *Basic linear algebra subprograms for Fortran usage*, ACM Trans. Math. Soft. **5**, No. 3, 308–323 (1979).
24. T. von Clarmann, M. Hopfner, B. Funke, M. Lopez-Puertas, A. Dudhia, V. Jay, F. Schreier, M. Ridolfi, S. Ceccherini, B.J. Kcrridgc, J. Reburn, and R. Siddans, *Modeling of atmospheric mid-infrared radiative transfer: The AMIL2DA algorithm intercomparison experiment*, J. Quant. Spectrosc. Radiat. Transfer (2002) (in press).
25. S. Buehler, C. Emde, P. Eriksson, C. Jiminez, Y. Kasai, G. Kopp, N. Koulev, T. Kuhn, O. Lemke, C. Melsheimer, J. Miao, D. Murtagh, S. Ochiai, F. Schreier, Ö.K. Sreerekha, N. Takahashi, S. Tsujimaru, J. Urban, V.O. John, and C. Verdes, *Intercomparison of radiative transfer models* (2002) (manuscript in preparation).
26. P.E. Gill, W. Murray, and M.H. Wright, *Practical Optimization* (Academic Press, London, UK, 1981).
27. A. Griewank and G. Corliss, eds., *Automatic Differentiation of Algorithms* (SIAM, Philadelphia, PA, 1991).
28. A. Griewank, *Evaluating Derivatives: Principles and Techniques of Algorithmic Differentiation* (SIAM, Philadelphia, PA, 2000).
29. Ch. Bischof, P. Khadmi, A. Maucr, and A. Carle, *Adifor 2.0: Automatic differentiation of Fortran 77 programs*, Computational Science & Engineering **3**, No. 3, 18–32 (1996).
30. T. Ernst, T. Rother, F. Schreier, J. Wauer, and W. Balzcr, *DLR's Virtual Lab: Scientific software just a mouse click away*, Computing in Science & Engineering **5**, No. 1 (2003).
31. G.P. Stiller, T. von Clarmann, B. Funke, N. Glatthor, F. Hase, M. Hopfner, and A. Linden, *Sensitivity of trace gas abundances retrievals from infrared limb emission spectra to simplifying approximations in radiative transfer modelling*, J. Quant. Spectrosc. Radiat. Transfer **72**, 249–280 (2002).